

# Crystalline and Glassy Phases in the Ternary System Tl/Bi/Cl: Synthesis and Crystal Structures of the Thallium(I) Chloridobismutates(III) $\text{Tl}_3\text{BiCl}_6$ and $\text{TlBi}_2\text{Cl}_7$

Johannes Beck<sup>\*[a]</sup> and Sebastian Benz<sup>[a]</sup>

*Dedicated to Professor Rüdiger Kniep on the Occasion of His 65th Birthday*

**Keywords:** Thallium; Chloridobismutates; Lone pair effect; NMR spectroscopy; X-ray absorption spectroscopy; Glass formation

**Abstract.** Slow cooling of melts composed of  $\text{TlCl}$  and  $\text{BiCl}_3$  allows for the isolation of the compounds  $\text{Tl}_3\text{BiCl}_6$  (**1**) and  $\text{TlBi}_2\text{Cl}_7$  (**2**). Compound **1** is formed by sublimation at 480 °C from the black melt of 3  $\text{TlCl}$  + 1  $\text{BiCl}_3$  as colourless crystals. The crystal structure determination (tetragonal,  $P4_2/m$ ) consists of nearly regular octahedral  $[\text{BiCl}_6]^{3-}$  anions and two independent  $\text{Tl}^+$  cations, which have coordination number 8 in form of a slightly distorted cube and 10 in form of an *Edshamar* polyhedron, respectively. The structure is not isotypic with the recently reported naturally occurring form of  $\text{Tl}_3\text{BiCl}_6$ , the mineral steropesite. Compound **2** is obtained from a dark red melt of composition  $\text{TlCl} + 2 \text{BiCl}_3$ . On rapid cooling, this melt solidifies to a metastable

dark red glass which at ambient temperature crystallises to a light amber crystalline powder within some weeks. The structure of **2** was determined by powder diffraction (triclinic,  $P\bar{1}$ ). A distinct lone pair effect is present causing an irregular coordination on the two independent bismuth atoms. Taking Bi–Cl bonds up to 3.5 Å into account, both bismuth atoms gain coordination number seven.  $^{203}\text{Tl}$  and  $^{205}\text{Tl}$  solid state NMR and XANES spectra on the Bi and Tl-L<sub>III</sub> edges of both glassy and crystalline  $\text{TlBi}_2\text{Cl}_7$  show that a close structural similarity exists between both forms. In contrast, the Raman spectra show distinct differences in the bands of the Bi–Cl vibrations region.

## Introduction

The crystal chemistry of the halides of trivalent bismuth is strongly influenced by the stereochemical activity of the lone electron pair on  $\text{Bi}^{3+}$ . Its structural influence is generally strong among the fluorides, but decreases with the heavier halogens. In the structure of  $\text{BiF}_3$ , the  $\text{Bi}^{3+}$  ion has a distorted square-antiprismatic coordination [1]. In  $\text{BiCl}_3$ , a strongly distorted 3+3 octahedral coordination with three short and three long Bi–Cl bonds is present [2], whereas for  $\text{BiI}_3$  an almost undistorted octahedral coordination environment was found [3]. During the last two decades, a number of alkali halogenidobismutates have been characterised, which show a large structural variability, mainly caused by the absence or presence of the lone-pair effect of the trivalent bismuth atoms. Examples are  $\text{CsBi}_2\text{F}_7$  [4] containing a Bi/F framework, in which the bismuth atoms have a strongly distorted six to eight fold coordination by fluoride anions. On the other hand, the structure of  $\text{Cs}_3\text{BiCl}_6$  [5] contains discrete  $\text{BiCl}_6$  units in which the Bi–Cl coordination is nearly ideally octahedral.

This structural variability can be further expanded by the substitution of alkali ions by such ions which themselves have

a potentially steric active lone-pair. Looking for substances with nonlinear optical properties, Hagemann and Weber prepared crystals of the compounds  $\text{Tl}_7\text{Bi}_3\text{I}_{16}$  and  $\text{Tl}_3\text{BiI}_6$ . The crystal structures, however, could not be determined due to twinning problems [6]. Later, Ruck and co-workers were able to characterise structurally the phases  $\text{Tl}_7\text{Bi}_3\text{I}_{16}$ ,  $\text{Tl}_3\text{BiI}_6$  [7], and  $\text{Tl}_3\text{Bi}_2\text{I}_9$  [8] by X-ray diffraction. All three iodidobismutates have bismuth in sixfold coordination. The  $\text{BiI}_6$  coordination octahedra are distorted, which is assigned to the effect of the lone pair.

Only one compound in the ternary system Tl/Bi/Cl was described so far. The mineral steropesite of the approximated formula  $\text{Tl}_3\text{BiCl}_6$  was recently found in volcanic high-temperature fumaroles [9]. The lack of knowledge on this ternary system led us to explore the formation and structures of phases among the thallium chloridobismutates.

## Experimental Section

### Starting Materials

$\text{BiCl}_3$  was obtained by chlorination of bismuth at 400 °C followed by several cycles of sublimation in vacuo.  $\text{TlCl}$  was precipitated from an aqueous solution of  $\text{TlNO}_3$  with hydrochloric acid, washed with water and dried in dynamic vacuum for several days. Glass ampoules of 10 cm length and 1.5 cm diameter were used as reaction vessels. All manipulations with the hygroscopic  $\text{BiCl}_3$  including charging and opening of the reaction ampoules were performed in an argon filled glove box.

\* Prof. Dr. J. Beck  
E-Mail: j.beck@uni-bonn.de

[a] Institut für Anorganische Chemie  
Universität Bonn  
Gerhard-Domagk-Str. 1  
53121 Bonn, Germany

### Synthesis of $\text{Tl}_3\text{BiCl}_6$

$\text{Tl}_3\text{BiCl}_6$  was synthesised by heating a melt of  $\text{TlCl}$  and  $\text{BiCl}_3$  in 3:1 molar ratio to 480 °C for ten hours in evacuated glass ampoules and slow cooling ( $5\text{ °C}\cdot\text{h}^{-1}$ ) the black-brown melt to ambient temperature. In a typical experiment, an ampoule of 12 cm length and 1.5 cm diameter was loaded with the  $\text{TlCl}/\text{BiCl}_3$  mixture (700 mg). Besides a black amorphous residue, colourless crystals of high refractivity deposited at the inner walls of the ampoule in the cooler region above the melt.

### Synthesis of $\text{TlBi}_2\text{Cl}_7$

Polycrystalline samples of  $\text{TlBi}_2\text{Cl}_7$  were prepared by heating a mixture of  $\text{TlCl}$  and  $\text{BiCl}_3$  in the molar ratio 1:2 to 250 °C in evacuated glass ampoules and slowly cooling ( $10\text{ °C}\cdot\text{h}^{-1}$ ) the dark red melt to ambient temperature. Trying to obtain single crystals by sublimation of the product only lead to sublimation of  $\text{BiCl}_3$  leaving behind the less volatile  $\text{TlCl}$ .

### Analytical Methods

Raman spectra were recorded using a BRUKER FT Raman spectrometer RFS100 in backscattering geometry, a Nd:YAG laser ( $\lambda = 1036\text{ nm}$ ) and a resolution of  $4\text{ cm}^{-1}$ . The laser power was adjusted between 30 and 300 mW. Measurements were done on powdered samples enclosed in sealed glass capillaries of 1 mm diameter. X-ray absorption spectra were measured at the synchrotron light source ANKA of the Forschungszentrum Karlsruhe, Germany. Solid state NMR spectra were recorded with a VARIAN Infinity Plus spectrometer applying the MAS

technique. Samples were packed in a rotor of 4 mm diameter and a rotation frequency of 12 kHz was applied. The spectrum was calibrated against a solution of  $\text{TlNO}_3$  with a concentration of  $0.1\text{ mol}\cdot\text{L}^{-1}$ . The resonance frequencies were 229.36 MHz for  $^{203}\text{Tl}$  and 231.62 MHz for  $^{205}\text{Tl}$ . Differential scanning calorimetry measurements were carried out with a DSC 204 Phoenix instrument (Netzsch Inc.) in closed aluminium crucibles with samples of about 15 mg.

### Crystal Structure Determination of $\text{Tl}_3\text{BiCl}_6$

The crystals of  $\text{Tl}_3\text{BiCl}_6$ , deposited from the gas phase as described above, were notoriously multiple twinned with diffraction patterns that could not be indexed and it took several attempts until a suitable single crystal specimen was found. Diffraction data were recorded at ambient temperature using a Bruker Nonius Kappa-CCD diffractometer with  $\text{Mo-K}_\alpha$  radiation. The tetragonal symmetry and the systematic absences led to the space group  $P4_2/m$ . An empirical absorption correction was applied to the data set [10]. The structure model was obtained by direct methods and refined based on  $F^2$  with anisotropic displacement parameters for all atoms [11]. The crystallographic data and details of data collection are summarised in Table 1, atomic coordinates in Table 2. The powder diffractograms of bulk samples can, however, be completely indexed and simulated on the basis of the tetragonal unit cell and the positional parameters obtained by the single crystal structure analysis. No reflections of additional phases are present indicating that under the applied reaction conditions only one single phase is formed.

**Table 1.** Crystallographic data and details of the structure determination for  $\text{Tl}_3\text{BiCl}_6$  and  $\text{TlBi}_2\text{Cl}_7$ .

Compound	$\text{Tl}_3\text{BiCl}_6$	$\text{TlBi}_2\text{Cl}_7$
Formula	$\text{BiCl}_6\text{Tl}_3$	$\text{Bi}_2\text{Cl}_7\text{Tl}$
Crystal system, space group	tetragonal, $P4_2/m$	triclinic, $P\bar{1}$
Number of formula units, $Z$	2	2
$a/\text{Å}$	8.9690(2)	8.8832(1)
$b/\text{Å}$		10.7632(1)
$c/\text{Å}$	7.4876(2)	6.9329(1)
$\alpha/^\circ$		107.523(1)
$\beta/^\circ$		107.334(1)
$\gamma/^\circ$		75.684(1)
$V/\text{Å}^3$	602.32(2)	594.30(1)
Density (calcd.) $/\text{g}\cdot\text{cm}^{-3}$	5.706	4.86
Absorption coefficient $\mu/\text{mm}^{-1}$	55.84 ( $\text{Mo-K}_\alpha$ )	96.89 ( $\text{Cu-K}_\alpha$ )
Diffractometer type	Bruker-Nonius $\kappa$ -CCD	Bruker D8 Advance
Radiation, wavelength $/\text{Å}$	$\text{Mo-K}_\alpha$ , 0.7107	$\text{Cu-K}_\alpha$ , 1.540598
Temperature $/\text{K}$	293	293
$2\theta_{\text{max}}/^\circ$	54.94°	$4^\circ < 2\theta < 81^\circ$
$hkl$ range	$h\pm 11, k\pm 8, l\pm 9$	$0 \leq h \leq 7, -8 \leq k \leq 9, -5 \leq l \leq 5$
Absorption correction	empirical [9]	cylinder correction
$T_{\text{min}}/T_{\text{max}}$	0.005/0.065	0.060/0.107
Reflections collected	1356	1484
Independent reflections, $R_{\text{merg}}$	730, 0.027	
No. of data and parameters	730 and 31	1480 and 41
Goodness-of-fit on $F^2$	1.066	1.55
$wR(F^2)$	0.070	0.043
$R( F )$ for $[n] F_o > 4\sigma(F_o)$	0.028 [682]	
$R( F )$ for all data	0.031	
$R_{\text{profiles}}$		0.031
$wR_{\text{profiles}}$		0.043
$wR(F^2)$		0.079
Largest difference peak and hole $/e\cdot\text{Å}^{-3}$	+1.30 and −1.57	+1.88 and −1.61

**Table 2.** Positional coordinates and equivalent isotropic displacement parameters  $U_{\text{eq}}/\text{\AA}^2$  for the atoms in the structure of  $\text{Ti}_3\text{BiCl}_6$ . Standard deviations refer to the last significant digit.

Atom	<i>x</i>	<i>y</i>	<i>z</i>	$U_{\text{eq}}$
Tl(1)	0.07685(7)	0.26533(6)	0	0.0540(3)
Tl(2)	0.5	0.5	0	0.0373(3)
Bi	0	0.5	0.5	0.0221(2)
Cl(1)	0.2037(2)	0.5612(3)	0.2463(3)	0.0382(5)
Cl(2)	0.0644(4)	0.2068(4)	0.5	0.059(1)

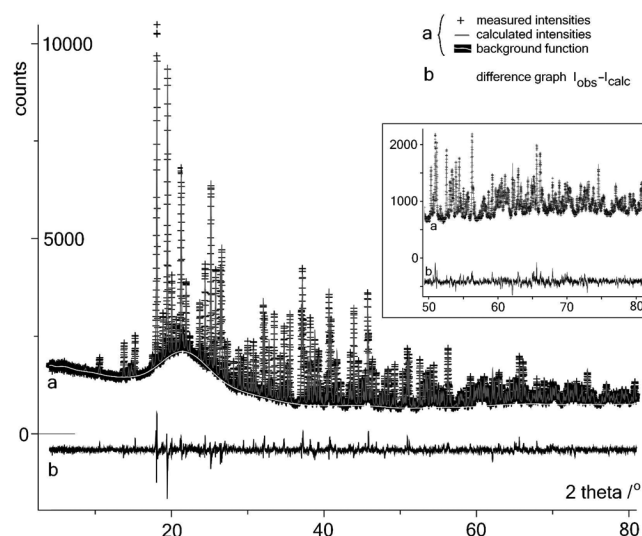
### Crystal Structure Determination of $\text{TiBi}_2\text{Cl}_7$

To protect the slightly hygroscopic powder of  $\text{TiBi}_2\text{Cl}_7$  from moisture, samples were filled in glass capillaries with a diameter of 0.2 mm after thoroughly grinding with an equal amount of glass powder. Data were collected at ambient temperature using a Bruker-D8 Advance powder diffractometer with  $\text{Cu-K}\alpha$  radiation. 10482 data points were recorded in the  $2\theta$  range 4 to  $81^\circ$  with increments of  $0.00735^\circ$ . Indexing of the diffractogram and determination of the lattice parameters were performed using the program WinXPow [12]. The diffraction pattern could be indexed by a triclinic cell. A first kind Chebyshev background function with 30 terms was applied as implemented in the GSAS program system [13]. A Pseudovoigt function with 18 terms was used to fit the reflection profiles for all 1480 identified reflections. Structure models were obtained with the aid of the program Endeavour [14]. Due to the closely similar atom scattering factors of bismuth and thallium, it turned out to be advantageous to assume both kinds of atoms as occupied by Pb in the structure solution process and in the early stages of refinement. Out of the suggested structure models those were chosen fulfilling the restraints  $d_{\text{min}}(\text{Pb-Pb}) = 3.5 \text{ \AA}$ ,  $d_{\text{min}}(\text{Pb-Cl}) = 2.5 \text{ \AA}$ ,  $d_{\text{min}}(\text{Cl-Cl}) = 3.0 \text{ \AA}$ . Eliminating all models with high coordination numbers of cations by cations or anions by anions, one centrosymmetric model was left, which was refined by the Rietveld method using the program GSAS [12]. Finally, an assignment of the different thallium and bismuth positions could be made unequivocally based on the respective cation-Cl bond lengths. Isotropic displacement parameters for all atoms were chosen and refined as free parameters. Table 1 contains the crystallographic data and details of the refinement, Table 3 the positional parameters of the atoms. Figure 1 shows the observed and the calculated powder diffractogram.

**Table 3.** Positional coordinates and isotropic displacement parameters  $U_{\text{iso}}/\text{\AA}^2$  for the atoms in the structure of  $\text{TiBi}_2\text{Cl}_7$ . Standard deviations refer to the last significant digit.

Atom	<i>x</i>	<i>y</i>	<i>z</i>	$U_{\text{iso}}$
Tl	0.6739(2)	0.1409(2)	0.9225(3)	0.0437(7)
Bi(1)	−0.2437(2)	0.5188(2)	0.5569(3)	0.0156(5)
Bi(2)	0.1380(2)	0.1583(2)	0.6966(2)	0.0209(6)
Cl(1)	−0.158(1)	0.3547(9)	0.795(1)	0.030(3)
Cl(2)	0.000(1)	0.0194(8)	0.262(1)	0.023(3)
Cl(3)	0.352(1)	0.318(1)	0.705(2)	0.053(4)
Cl(4)	0.256(1)	0.1904(9)	1.094(1)	0.032(3)
Cl(5)	0.370(1)	−0.0332(8)	0.647(1)	0.024(3)
Cl(6)	0.053(1)	0.6431(8)	0.648(1)	0.027(3)
Cl(7)	−0.445(1)	0.3869(9)	0.311(1)	0.028(3)

Further details on the crystal structure investigations may be obtained from the Fachinformationszentrum Karlsruhe, 76344 Eggenstein-Leopoldshafen, Germany (Fax: +49-7247-808-666; E-Mail: crysdata@fiz-karlsruhe.de), on quoting the depository numbers CSD-421317 for

**Figure 1.** Powder diffractogram of  $\text{TiBi}_2\text{Cl}_7$ . Shown are the measured intensities, the calculated intensities, the background function, and the difference curve  $I_{\text{obs}} - I_{\text{calc}}$ . The inset shows an enlarged view of the high angle region of the diffractogram.

$\text{Ti}_3\text{BiCl}_6$  and CSD-421318 for  $\text{TiBi}_2\text{Cl}_7$  [15]. The graphical representations were drawn with the use of the programs DIAMOND [16] and POV-RAY [17].

## Results and Discussion

### Synthesis of Thallium(I) Chloridobismutates

In a series of experiments, the formation of discrete phases in the ternary system Tl/Bi/Cl was investigated by reactions of  $\text{TlCl}$  and  $\text{BiCl}_3$  in different molar ratios from 3:1 to 1:3. With intermediate compositions no formation of compounds was observed. Powder diffractograms of solidified melts of compositions between 2:1 and 1:1 showed beside reflections of new phases reflections of the starting materials  $\text{TlCl}$  and  $\text{BiCl}_3$ . Another common feature is the widespread formation of dark coloured glassy solids on solidification of the melts. The formation of ternary compounds was only observed on the border areas of the investigated compositions, in the thallium rich and the bismuth rich region. Two different thallium(I) chloridobismutates,  $\text{Ti}_3\text{BiCl}_6$  and  $\text{TiBi}_2\text{Cl}_7$ , composed of  $\text{TlCl}$  and  $\text{BiCl}_3$  in the stoichiometric amounts 3:1 and 1:2, could be synthesised and isolated as discrete phases. With both compositions as a typical feature dark coloured melts are formed. In the case of the 3:1 mixture, the deposition of crystals of  $\text{Ti}_3\text{BiCl}_6$  from the gas phase above the melt in a small temperature gradient during the slow cooling process from  $480^\circ\text{C}$  to ambient temperature could be achieved. The deposited colourless crystals of  $\text{Ti}_3\text{BiCl}_6$  are strongly light refracting. The analogous experiments with melts of the composition 1  $\text{TlCl}$ :2  $\text{BiCl}_3$  gave melts of dark-red colour. In contrast to the  $\text{TlCl}$  rich melts, no deposition of crystalline material was observed from the gas phase above the melts of this composition. Slow cooling of such a melt from  $250^\circ\text{C}$  to ambient temperature gives an amber coloured microcrystalline solid. By rapid quenching the melt from

250 °C to –38 °C, performed by immersing the hot reaction ampoule into chilled liquid mercury, an amorphous, glassy, transparent, dark-red product was isolated (Figure 2a). Grinding of the red glass gives a light red to rose powder. The non-crystallinity was verified by X-ray powder diffraction. Leaving this glassy material at room temperature under protection from moist air causes the slow conversion into the light amber coloured crystalline phase (Figure 2b).

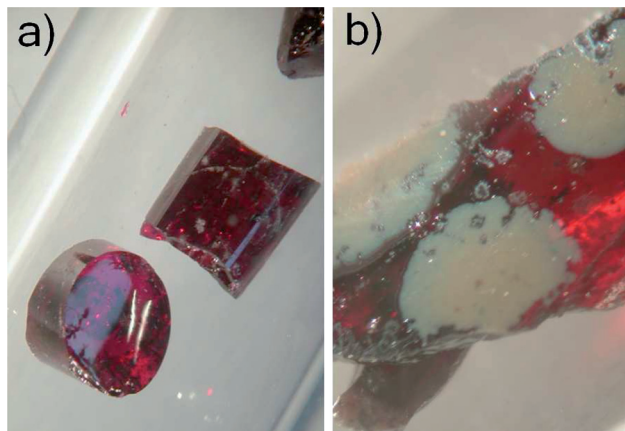


**Figure 2.** Photographs of pieces of the rapidly cooled melt of  $\text{TiBi}_2\text{Cl}_7$ , forming a dark red, transparent glass (a), and this glass after two weeks at room temperature with emerging amber coloured crystalline segregations (b).

### Crystal Structure of $\text{Ti}_3\text{BiCl}_6$

The tetragonal unit cell of  $\text{Ti}_3\text{BiCl}_6$  contains two formula units (Figure 3). Two bismuth atoms occupying the site symmetry  $2/m$  are almost regular octahedrally coordinated by six chlorine atoms. The two independent Bi–Cl distances are equal within standard deviations and amount 2.692(2) and 2.693(3) Å (Table 4). The angular distortions within the  $\text{BiCl}_6$  octahedra are small. A significant deviation from rectangularity is observed for the plane containing the bismuth atoms and the four Cl(1) atoms, which is inclined by 3° to the Cl(2)–Bi–Cl(2<sup>II</sup>) axis. An almost regular shape of  $\text{BiCl}_6$  octahedra in the structures of chloridobismutates(III) is not unusual and found e.g. in the structure of  $(\text{NH}_4)_3[\text{BiCl}_6]$  (Bi–Cl 2.682 to 2.753 Å, angle deviations from 90° less than 6°) [18].

The tetragonal unit cell of  $\text{Ti}_3\text{BiCl}_6$  contains two independent thallium atoms. The coordination sphere around the Tl(1) atoms, located on the *Wyckoff* site 4j in the mirror plane may be described best by a distorted *Edshamar* polyhedron with coordination number of 10 and Tl–Cl distances in the region between 3.117(3) to 3.802(3) Å, formally built by half a cube and half an icosahedron. Tl(2) atoms with site symmetry  $2/m$  are surrounded by eight chlorine atoms in shape of a cube. The actual reduction of the ideal cubic symmetry to  $2/m$  allows for distortions which find their expressions in two different Tl–Cl distances of 3.281(3) and 3.312(3) Å. The cuboidal Tl(2)Cl<sub>8</sub> polyhedra are condensed to linear strands along the crystallographic *c* axis with the thallium ions being half the length of

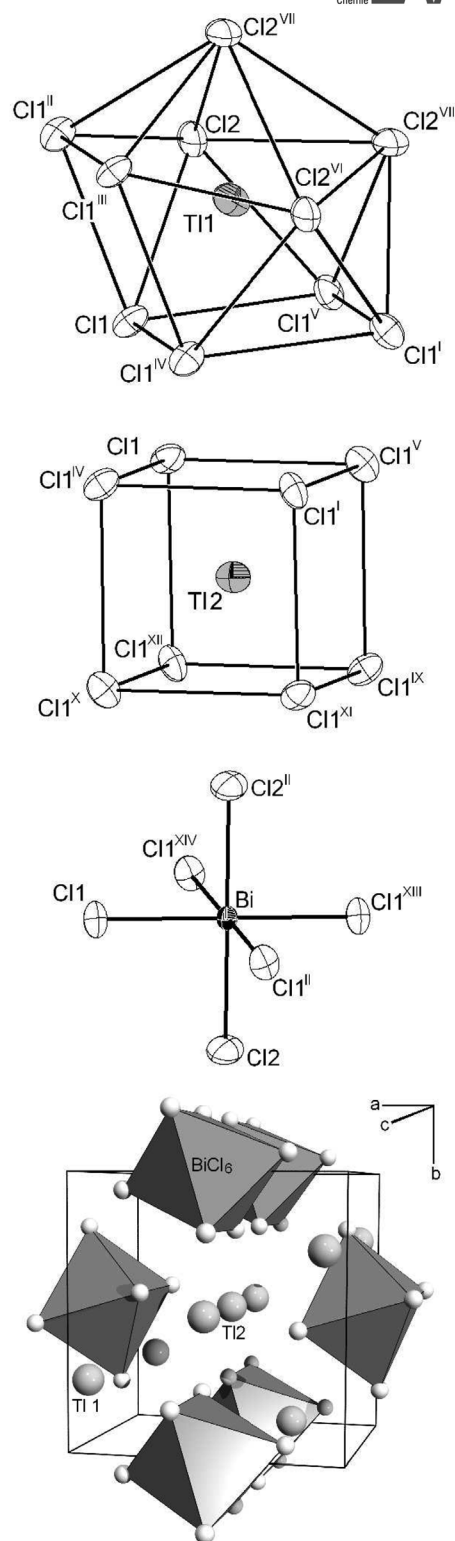


**Figure 3.** Details of the crystal structure of  $\text{Ti}_3\text{BiCl}_6$  (from top to bottom): The coordination polyhedra of the two independent  $\text{Tl}^+$  ions Tl(1) and Tl(2), the octahedral  $[\text{BiCl}_6]^{3-}$  anion, and a view of the unit cell along the crystallographic *c* axis. Thermal ellipsoids are drawn to include a probability density of 50 %. Symmetry operations: I: 1 –*y*, *x*, –0.5+*z*; II: –*x*, 1 –*y*, *z*; III: –*x*, 1 –*y*, –*z*; IV: *x*, *y*, –*z*; V: 1 –*y*, *x*, 0.5–*z*; VI: *x*, *y*, –1+*z*; VII: –*y*, *x*, –0.5+*z*; VIII: *y*, –*x*, –0.5+*z*; IX: 1 –*x*, 1 –*y*, *z*; X: *y*, 1 –*x*, –0.5+*z*; XI: 1 –*x*, 1 –*y*, –*z*; XII: *y*, 1 –*x*, 0.5–*z*; XIII: –*x*, 1 –*y*, 1 –*z*; XIV: *x*, *y*, 1 –*z*.



**Table 4.** Selected bond lengths /Å in the structures of  $\text{Ti}_3\text{BiCl}_6$  and  $\text{TiBi}_2\text{Cl}_7$ . For symmetry operations see legends of Figure 1 and Figure 2.

$\text{Ti}_3\text{BiCl}_6$		$\text{TiBi}_2\text{Cl}_7$	
Bi–Cl(1), Cl(1 <sup>II</sup> ), Cl(1 <sup>XIII</sup> ), Cl(1 <sup>XIV</sup> )	2.692(2)	Bi(1)–Cl(1)	2.603(9)
Bi–Cl(2), Cl(2 <sup>II</sup> )	2.693(3)	Bi(1)–Cl(3 <sup>II</sup> )	2.705(9)
Tl(1)–Cl(1), Cl(1 <sup>IV</sup> )	3.426(3)	Bi(1)–Cl(4 <sup>I</sup> )	3.331(9)
Tl(1)–Cl(1 <sup>II</sup> ), Cl(1 <sup>III</sup> )	3.486(3)	Bi(1)–Cl(6)	3.059(9)
Tl(1)–Cl(1 <sup>I</sup> ), Cl(1 <sup>V</sup> )	3.802(3)	Bi(1)–Cl(6 <sup>II</sup> )	2.533(9)
Tl(2)–Cl(1), Cl(1 <sup>IV</sup> ), Cl(1 <sup>IX</sup> ), Cl(1 <sup>XI</sup> )	3.281(3)	Bi(1)–Cl(7)	2.470(9)
Tl(2)–Cl(1 <sup>I</sup> ), Cl(1 <sup>V</sup> ), Cl(1 <sup>X</sup> ), Cl(1 <sup>XII</sup> )	3.312(3)	Bi(1)–Cl(7 <sup>III</sup> )	3.010(9)
		Bi(2)–Cl(1)	3.048(10)
		Bi(2)–Cl(2)	2.967(8)
		Bi(2)–Cl(2 <sup>IV</sup> )	2.636(8)
		Bi(2)–Cl(3)	2.845(10)
		Bi(2)–Cl(4)	2.584(9)
		Bi(2)–Cl(5)	2.551(8)
		Bi(2)–Cl(6 <sup>II</sup> )	3.467(9)
		Tl–Cl	3.374(9) to 4.087(9)

the *c* axis (3.744 Å) apart. The  $\text{Tl}(1)\text{Cl}_{10}$  polyhedra share two of their square faces and four edges with the  $\text{Tl}(2)\text{Cl}_8$  polyhedra resulting in a three-dimensional network (Figure 3).

Since  $\text{Ti}_3\text{BiCl}_6$  is of the basic formula type  $A_3BX_6$ , for which numerous representatives are known, we attempted to contribute its structure to a known structure type. The actual release of the ICSD database [19] contains 479 known crystal structures of this formula type. Using the subroutine CMPZ of the program KPLOTT [20] a similarity search was performed. The tolerances were set to high values: for all lattice constants a tolerance of  $\pm 15\%$ , for deviation of angles  $\pm 5\%$ , the inclusion spheres for atom positions were enlarged to 1.0 Å. Surprisingly and despite the wide tolerances, no coincidence with any of the deposited structures of the  $A_3BX_6$  formula type compounds was found. The arrangement of the  $\text{Tl}^+$  ions in rows along one crystallographic axis with the remarkably short  $\text{Tl}^+\cdots\text{Tl}^+$  distances is unusual and causes the uniqueness of  $\text{Ti}_3\text{BiCl}_6$  within the structures of this formula type.

The recently described mineral steropesite was discovered as yellow crystals of the formula  $\text{Ti}_3\text{BiCl}_6$  [9]. The structure was solved on a crystal containing 10 % bromine on the chlorine positions. It crystallises in the monoclinic system with a very large unit cell having a volume of almost 5000 Å<sup>3</sup>. Its crystal structure consists of discrete and slightly distorted octahedral  $[\text{BiCl}_6]^{3-}$  anions and  $\text{Tl}^+$  cations with coordination numbers between six and eight. The reported structure can be considered as a distorted variant of the structure of  $\text{Cs}_3\text{BiCl}_6$ , but besides the presence of the analogous building units there is no direct relation to the tetragonal form of  $\text{Ti}_3\text{BiCl}_6$  reported here.

### High Temperature Phase of $\text{Ti}_3\text{BiCl}_6$

The thermal behaviour of  $\text{Ti}_3\text{BiCl}_6$  was investigated in the temperature region between ambient temperature and 400 °C by differential scanning calorimetry at a heating rate of 10 °C·min<sup>−1</sup>. Two reproducible, endothermic effects could be detected, a solid state phase transition at 189.1 °C (0.93 kJ·mol<sup>−1</sup>), and the melting at 378.4 °C (3.4 kJ·mol<sup>−1</sup>). To

test for a transition into a high temperature form, crystals of the low temperature form were grinded to a powder, filled into a glass capillary, which was sealed, and investigated by X-ray powder diffractometry. Above 230 °C the diffraction pattern changed completely and the reflections of the room temperature phase disappeared. Lowering the temperature again to 180 °C caused only an incomplete reconversion since the diffractogram of the room temperature phase appeared again but the strongest reflections of the high temperature diffractogram remained. The powder diffractogram at high temperature shows a significant higher number of reflections. This behaviour may indicate a transition to a high temperature phase with a structure of lower symmetry. On looking for a structure model for the assumed high temperature phase, we found that the calculated powder diffractogram of monoclinic  $\text{Cs}_3\text{BiCl}_6$ , after substitution of caesium against thallium, shows a striking similarity to the diffractogram of HT- $\text{Ti}_3\text{BiCl}_6$ . The complete indexing of the diffractogram was not successful and a refinement of the structure model was not possible on basis of the observed diffraction data. We cannot, however, rule out the possibility of a partial decomposition of the sample.

### Crystal Structure of $\text{TiBi}_2\text{Cl}_7$

The triclinic unit cell of  $\text{TiBi}_2\text{Cl}_7$  contains two formula units with all atoms occupying general positions. The coordination of the two independent bismuth atoms and the thallium atom by surrounding Cl atoms is much more irregular in comparison to the structure of  $\text{Ti}_3\text{BiCl}_6$ . In Figure 4 the distribution of these distances is depicted in the form of histograms. For all three independent cations present in the crystal structure, a distinct gap is observed which allows for the definition of coordination polyhedra. The two bismuth atoms both gain coordination number seven with all Bi–Cl distances up to 3.34 Å for Bi(1) and 3.47 Å for Bi(2) taken into account. In each of the two  $\text{BiCl}_7$  polyhedra one Cl atom achieves a long distance which is typical for a pronounced lone pair effect of the three-valent bismuth atom. The  $\text{BiCl}_7$  polyhedra are connected by common corners and edges to a three dimensional net, in

which the  $\text{Tl}^+$  ions are embedded. Thallium gains the coordination number eleven if all  $\text{Tl}-\text{Cl}$  distances up to 4.09 Å are considered (Figure 4).

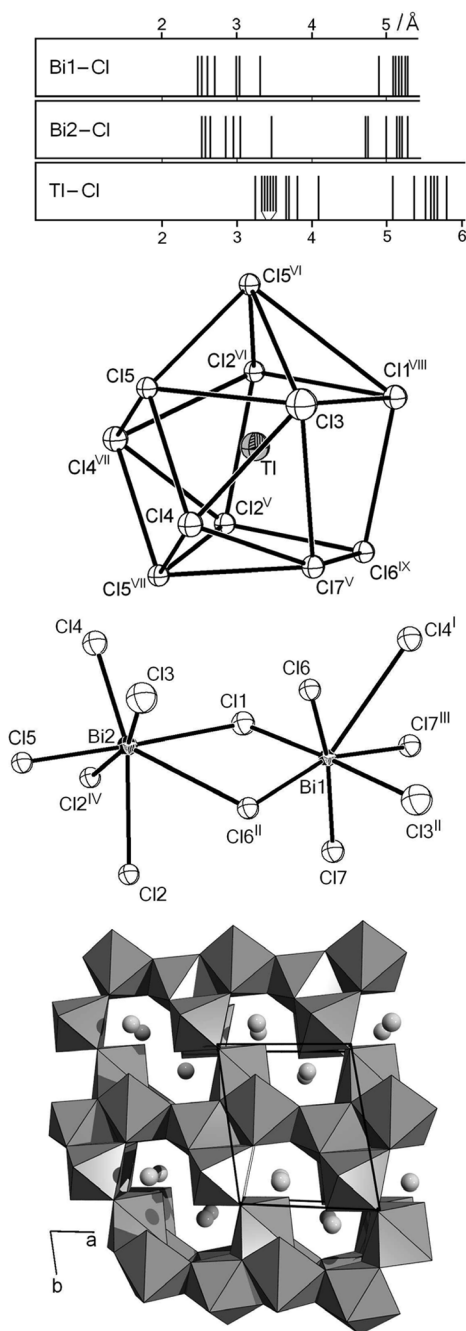


**Figure 4.** Details of the crystal structure of  $\text{TlBi}_2\text{Cl}_7$  (from top to bottom): The  $\text{Bi}-\text{Cl}$  and  $\text{Tl}-\text{Cl}$  distances in the form of histograms, the coordination polyhedron of the  $\text{Tl}^+$  ion, the coordination of the two independent bismuth atoms  $\text{Bi}(1)$  and  $\text{Bi}(2)$ , and a view of the unit cell along the crystallographic  $c$  axis. In the two detailed representations, atoms are drawn as spheres with radii corresponding to 50 % of the probability density of the thermal vibration. Symmetry operations: I:  $-x, 1-y, 2-z$ ; II:  $-x, 1-y, 1-z$ ; III:  $-1-x, 1-y, 1-z$ ; IV:  $-x, -y, 1-z$ ; V:  $1+x, y, 1+z$ ; VI:  $1-x, -y, 1-z$ ; VII:  $1-x, -y, 2-z$ ; VIII:  $1+x, y, z$ ; IX:  $1-x, 1-y, 2-z$ .

### Vibrational Spectra

Of both compounds,  $\text{Tl}_3\text{BiCl}_6$  and  $\text{TlBi}_2\text{Cl}_7$ , Raman spectra were recorded. As expected, the spectrum of  $\text{Tl}_3\text{BiCl}_6$  shows only a low number of bands due to the high local symmetry of the vibrationally active  $\text{BiCl}_6$  group. Three broad bands at 261 (vs), 218 (s), and 117 (vs)  $\text{cm}^{-1}$  were observed. These bands are identical with those of  $\text{Cs}_3\text{BiCl}_6$  within the resolution limit and can be attributed to the fundamental Raman active vibrations  $A_{1g}$ ,  $E_g$ ,  $T_{2g}$  of the  $\text{BiCl}_6$  octahedron. In the region between 300 and 100  $\text{cm}^{-1}$  the Raman spectrum of  $\text{TlBi}_2\text{Cl}_7$  shows 10 bands (104(s), 116(m), 121(m), 132(s), 144(w), 172(s), 186(s), 247(s), 269(s), 290(s)  $\text{cm}^{-1}$ ). Due to the irregular, low symmetric coordination of the cation in this structure, a definite attribution of these bands cannot be made.

### Structural Investigations of Glassy $\text{TlBi}_2\text{Cl}_7$

The thermal behaviour of glassy  $\text{TlBi}_2\text{Cl}_7$  was measured in the temperature region between  $-20$  and  $230$   $^{\circ}\text{C}$ , the respective differential scanning calorimetry (DSC) function, obtained at a heating rate of  $10$   $^{\circ}\text{C}\cdot\text{min}^{-1}$  is given in Figure 5. The endothermic effect at  $41.3$   $^{\circ}\text{C}$  (point *a* in Figure 5,  $2.9$   $\text{kJ}\cdot\text{mol}^{-1}$ ) is attributed to the glass transition. The two following exothermic effects at  $59.3$  (*b* and *c*,  $-6.0$   $\text{kJ}\cdot\text{mol}^{-1}$ ) are attributed to crystallisation processes. The small endothermic effect at  $180$   $^{\circ}\text{C}$  (*d*) was not observable in all measurements and is probably an artefact. At  $189.5$   $^{\circ}\text{C}$  melting occurs (*e*,  $30.3$   $\text{kJ}\cdot\text{mol}^{-1}$ ). On cooling the samples after melting, a sharp exothermic signal at  $109$   $^{\circ}\text{C}$  appears (*f*,  $-22.1$   $\text{kJ}\cdot\text{mol}^{-1}$ ) originating from crystallisation of the melt. If the measurement is carried out with a lower heating rate of  $1$   $^{\circ}\text{C}\cdot\text{min}^{-1}$ , the glass transition shifts to  $35.2$   $^{\circ}\text{C}$ . According to the empirical relation  $T_g = A + B \log \beta$  with  $T_g$  = observed glass transition temperature,  $A$  = true glass transition temperature,  $B$  = empirical factor depending on the preparation of the glass,  $\beta$  = heating rate, the transition temperature at  $32.5$   $^{\circ}\text{C}$  is identical with the true transition temperature [21]. The relation of the absolute glass transition temperature to the melting temperature allows within limits for information on the structural properties of amorphous networks. For highly symmetric polymers made up from small monomeric units,  $T_g/T_m$  is generally 0.5 or lower, for the broad majority of polymers, however, this relation amounts 2/3 [22]. For the amorphous  $\text{TlBi}_2\text{Cl}_7$  phase  $T_g/T_m$  is  $308\text{ K}/463\text{ K} = 0.66$ . The observed thermal effects do thus not allow for detailed conclusions on the structural properties of the glass.

$^{205}\text{Tl}$  and  $^{203}\text{Tl}$  MAS solid state NMR spectra were recorded in order to find further insight into the structure of the red glassy form of  $\text{TlBi}_2\text{Cl}_7$ . The MAS spectra of both, the glassy and the crystalline  $\text{TlBi}_2\text{Cl}_7$  do not show differences. Only one broad signal centred at 47.7 ppm relative to the standard was observed (Figure 6). This is in line with the crystallographic cell, which contains only one symmetry-independent thallium atom. The similarity of the spectra suggests that the chemical environment of the thallium atoms in both phases does not show large differences.

The vibrational spectrum of the amorphous  $\text{TlBi}_2\text{Cl}_7$  phase shows, however, distinct differences to the spectrum of the

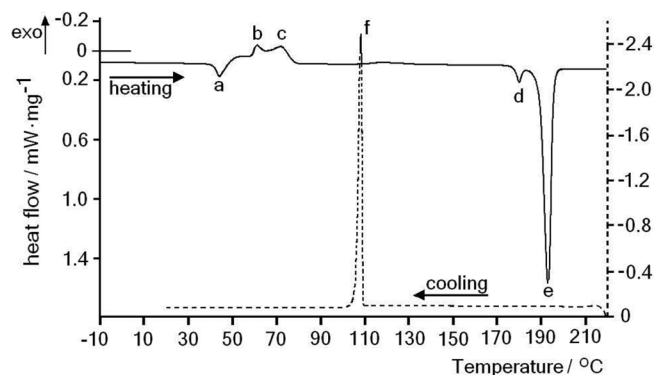


**Figure 5.** Differential scanning calorimetry function of  $\text{TlBi}_2\text{Cl}_7$ . The solid line represents the heating curve from  $-10$  to  $210$  °C, the dotted line the cooling process back to ambient temperature. The observable thermal effects are indicated by letters a–f, see text. The temperature rate for heating and for cooling was  $10$  °C·min $^{-1}$ .

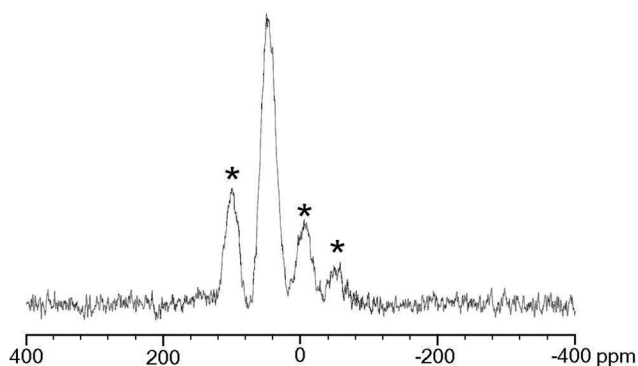


**Figure 6.**  $^{205}\text{Tl}$  MAS-NMR spectrum of amorphous  $\text{TlBi}_2\text{Cl}_7$  at  $12$  kHz spinning speed. Signals marked with an asterisk are rotational bands. The respective  $^{203}\text{Tl}$  spectrum is of almost identical shape but shows lower signal intensity.

crystalline form. Eight bands ( $126(\text{s})$ ,  $142(\text{m})$ ,  $157(\text{m})$ ,  $178(\text{s})$ ,  $246(\text{m})$ ,  $268(\text{w})$ ,  $292(\text{sh, s})$ ,  $306(\text{vs})$   $\text{cm}^{-1}$ ) are present, of which only three ( $142$ ,  $246$ ,  $268$   $\text{cm}^{-1}$ ) are observed at the same frequencies as for the crystalline state. The spectrum of amorphous  $\text{TlBi}_2\text{Cl}_7$  shows instead a close similarity to the spectrum of  $\text{BiCl}_3$  (six bands at  $280(\text{vs})$ ,  $262(\text{m})$ ,  $252(\text{sh, w})$ ,  $179(\text{m})$ ,  $141(\text{m})$ ,  $119(\text{m})$ ) in the frequency and intensity distribution. For  $\text{BiCl}_3$  the bands at  $280$  ( $A_1$ ) and  $252$   $\text{cm}^{-1}$  ( $E$ ) can be attributed to the  $C_{3v}$  symmetric molecules, which are present in the solid state. The vibrational spectra lead to the suggestion that amorphous  $\text{TlBi}_2\text{Cl}_7$  contains  $\text{BiCl}_3$  building units as present in the structure of crystalline  $\text{BiCl}_3$ .

Near edge X-ray absorption spectra (XANES) of  $\text{Tl}_3\text{BiCl}_6$ , and amorphous and crystalline  $\text{TlBi}_2\text{Cl}_7$  were recorded on both the  $\text{Tl-L}_{\text{III}}$  and the  $\text{Bi-L}_{\text{III}}$  edges. Figure 7 shows the spectra on the  $\text{Bi-L}_{\text{III}}$  edges as a superposition for all three samples. A striking similarity is observed between the spectra of glassy and crystalline  $\text{TlBi}_2\text{Cl}_7$ , whereas the spectrum of  $\text{Tl}_3\text{BiCl}_6$  is different throughout the entire energy interval. This observation is also valid for the spectra on the  $\text{Tl-L}_{\text{III}}$  edge. This result is in line with the solid state NMR spectra, indicating that

$\text{TlBi}_2\text{Cl}_7$  in the glassy and the crystalline state both have closely related coordination environments around the thallium and bismuth atoms. On the other hand, the Raman spectra with their differing patterns of vibrational bands indicate a substantially altered local structure.

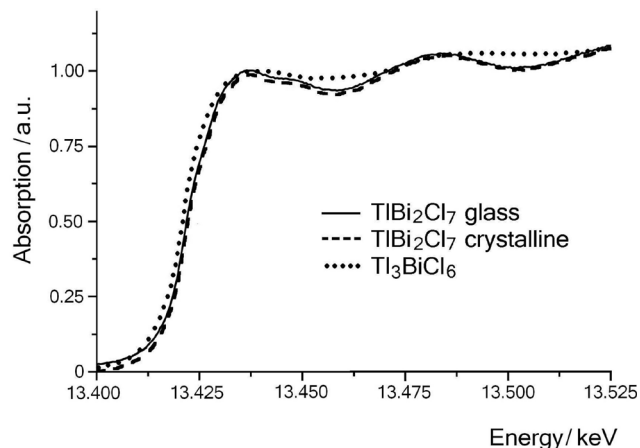


**Figure 7.** XANES spectrum on the  $\text{Bi-L}_{\text{III}}$  absorption edge of glassy and crystalline  $\text{TlBi}_2\text{Cl}_7$ , and of crystalline  $\text{Tl}_3\text{BiCl}_6$ .

## Conclusions

Two discrete phases were prepared and characterised in the ternary system  $\text{Tl/Bi/Cl}$ , both showing structural peculiarities. The  $\text{TlCl}$  rich compound  $\text{Tl}_3\text{BiCl}_6$  is built of only slightly distorted  $[\text{BiCl}_6]^{3-}$  octahedra, whereas the  $\text{BiCl}_3$  rich phase  $\text{TlBi}_2\text{Cl}_7$  is made of a complex network of connected, irregular  $\text{BiCl}_7$  polyhedra. In both structures, the  $\text{Tl}^+$  ions gain high coordination numbers between eight and eleven. A remarkable and yet not elucidated detail is the amorphous state of  $\text{TlBi}_2\text{Cl}_7$ , which forms a glass on rapid cooling of the melt. The metastable, transparent glass is of intensive dark-red colour, whereas the crystalline phase is almost colourless. No explanation for the colour of the glass could be found and the attempts to find structural relations between the glassy and the crystalline state by XANES, NMR and Raman spectra lead to contradictory results.

## Acknowledgement

We gratefully acknowledge the measurements of the X-ray absorption spectra by *N. Palina*, *B. Brendebach* and *H. Modrow*, the collection of the single crystal data by *J. Daniels*, the recording of the NMR spectra by *W. Hoffbauer* and the dedicated help of *R. Hundt* with the data base searches.

## References

- [1] O. Greis, M. Martinez-Ripoll, *Z. Anorg. Allg. Chem.* **1977**, 436, 105.
- [2] S. C. Nyburg, G. A. Ozin, J. T. Szymanski, *Acta Crystallogr., Sect. B* **1972**, 28, 2885.
- [3] M. Ruck, *Z. Kristallogr.* **1995**, 210, 650.

- [4] A. M. Golubev, B. A. Maksimov, R. K. Rastsvetaeva, *Crystallogr. Rep.* **1997**, 42, 243.
- [5] F. Benachenhou, G. Mairesse, G. Nowogrocki, D. Thomas, *J. Solid State Chem.* **1986**, 65, 13.
- [6] M. Hagemann, H. J. Weber, *Appl. Phys.* **1996**, A63, 67.
- [7] T. Aussieker, H. L. Keller, T. Oldag, Y. Prots, M. Ruck, A. Wosylus, *Z. Anorg. Allg. Chem.* **2007**, 633, 603.
- [8] A. Wosylus, U. Schwarz, M. Ruck, *Z. Anorg. Allg. Chem.* **2005**, 631, 1055.
- [9] F. Demartin, C. M. Gramaccioli, I. Campostrini, *Can. Mineralog.* **2009**, 47, 373.
- [10] Z. Otwinowski, W. Minor, Program SCALEPACK, *Macromol. Crystallogr. A* **1997**, 276, 307.
- [11] G. M. Sheldrick, *SHELX97 [includes SHELXS97, SHELXL97, CIFTAB]*, - Programs for Crystal Structure Analysis (Release 97–2), Universität Göttingen, Germany, **1998**.
- [12] *WinXPow*, Powder Diffraction Software, Stoe & Cie Ltd., Darmstadt, Germany, **1999**.
- [13] *General Structure Analysis System (GSAS)*, A. C. Larson, R. B. Von Dreele, Los Alamos National Laboratory, Report LAUR 86–748, **2000**.
- [14] *ENDEAVOUR, Program for Structure Solution from Powder Diffraction*, Crystal Impact GbR, Bonn, Germany, **1999**; H. Putz, J. C. Schoen, M. Jansen, *J. Appl. Crystallogr.* **1999**, 32, 864.
- [15] Detailed crystallographic data can be obtained from the *Fachinformationszentrum Karlsruhe* by quoting the deposit number, the names of the authors and the literature citation. Details about inquiries are given on [www.fzinformationsdienste.de](http://www.fzinformationsdienste.de).
- [16] *DIAMOND*, Molecular and Crystal Structure Visualisation Program, ver. 3.1, Crystal Impact GbR, Bonn, Germany, **2008**.
- [17] *POV-Ray*, Persistence of Vision Raytracer Pty. Ltd., Williamstown, Australia, **2004**.
- [18] I. Belkyl, R. Mokhlisse, B. Tanouti, K. F. Hesse, W. Depmeier, *Eur. J. Solid State Inorg. Chem.* **1997**, 34, 1085.
- [19] *Inorganic Crystal Structure Database ICSD*, Fachinformationszentrum FIZ Karlsruhe, Germany, Release **2009–1**.
- [20] *KPLOT*, Program for Graphical Representation and Analysis of Crystal Structures, R. Hundt, University of Bonn, Germany, **2007**.
- [21] A. A. Othman, K. A. Aly, A. M. Abousehly, *Solid State Commun.* **2006**, 138, 184.
- [22] H. K. Cammenga, M. Epple, *Angew. Chem.* **1995**, 107, *Angew. Chem. Int. Ed. Engl.* **1995**, 34, 1171.

Received: December 15, 2009  
Published Online: March 31, 2010